



Technical Sciences
Academy of Romania
www.jesi.astr.ro

Received 15 June 2018

Accepted 14 September 2018

Received in revised form 29 August 2018

Nanomaterials characterization by Mössbauer spectroscopy

ION BIBICU*

Technical Sciences Academy of Romania, Bucharest, Romania

Abstract. Mössbauer spectroscopy has one of its most important features the ability to undertake bulk of varying thickness using the secondary radiation emitted after resonant absorption of a gamma ray. Using emitted electrons it is possible to characterize the nanomaterials. It is a non-destructive technique that can be applied *in situ* investigations. A short description of the technique is given. The author presents the detectors achieved for these studies and the principal results in nanomaterial characterization. Few results are described more detailed.

Keywords: Mössbauer spectroscopy, electron Mössbauer spectroscopy (CEMS), proportional counters, nanomaterials, surface analyses, corrosion.

1. Introduction

Mössbauer spectroscopy [1] is based on the incorporation of the emitting and absorbing nuclei within a solid matrix, which enables resonant recoil free absorption and emission of γ -rays. Its importance lies in the very narrow line width of the emitting photon resulting from the relatively long lifetime of the excited nuclear state - typically of 10^{-8} s, corresponding to a natural line width of the order of 10^{-8} eV - and the consequent ability to probe the variations in nuclear energy levels resulting from any discrete changes in the chemical state and/or environment of the Mössbauer nucleus. Such changes in nuclear energy levels are measured by modifying the energy of the probing γ -rays by applying a Doppler shift: a Mössbauer spectrum therefore consists of a plot of counts against applied Doppler velocity (positive and negative). Significant recoil-free-fractions occur only for gamma energies less than 150 keV, and, as the energy of the gamma ray increases so also does the necessity of collecting data with the sample and/or source at low temperatures. This limitation obviously means that room or high temperature Mössbauer work is possible only for a limited number of elements, (e.g. ^{57}Fe , ^{119}Sn , ^{151}Eu).

*Correspondence address: ionbibicu10@gmail.com

Following resonant absorption of a gamma ray, the nucleus may de-excite by emission of a gamma ray or by the process of internal conversion where an inner (K or L) shell electron is emitted. Accompanying conversion electron emission is a characteristic X-ray emitted as a result of the repopulating of the inner energy levels. Detecting the three-backscattered particles permits surface studies to be performed. The conversion electron signal is quite high for the ^{57}Fe , ^{119}Sn and ^{151}Eu isotopes.

The normal transmission geometry investigates iron-containing samples of thickness typically < 30 microns. However, in scattering geometry surfaces, coatings and thin films can be studied on substrates and to various depths through the detection of emitted 7.3 keV conversion electrons, Conversion Electron Mössbauer Spectroscopy (CEMS), (0-250 nanometers), 6.4 keV X-rays, X-ray Mössbauer Spectroscopy (CXMS), (20 microns) and 14.4 keV gamma-rays, Gamma-ray Mössbauer Spectroscopy (GMS), (0-30 microns). Conversion electron energies emitted by ^{119}Sn , ^{151}Eu isotopes are closed of ^{57}Fe isotopes. ^{119}Sn emits 3.44-4.13 keV X-rays and ^{151}Eu emits 5.84-7.64 keV X-rays.

By means of the conversion electron detection Mössbauer spectroscopy became one of the methods for nanomaterials characterization. Without a doubt, surface is the most important part of a solid [2]. Mössbauer spectroscopy [2, 3] has as one of its most important features the ability to simultaneously undertake bulk and surface analyses. It is a non-destructive technique that can be applied *in situ* to investigate surface of varying thickness from thin films to coatings without the need to remove them from their substrate. It gives chemical, structural and magnetic characterization in a single experiment and can probe surfaces and buried interfaces as well on an atomically local scale. Mössbauer spectroscopy is one of the numerous methods for the analysis of the phase composition and the microstructure of materials. The Fe-57 is the most studied isotope followed by Sn-119 and Eu-151. The three isotopes studied by totalize more than 85% from publications. On the other part, it suffers from a lack of sensitivity and for the very thin surfaces and interfaces take too long acquisition times.

The paper presents the author contribution in nanomaterials characterization. The experimental devices for nanomaterials investigation were developed and representative results concerning nanomaterials studies, mainly, by using the Mössbauer spectroscopy, will be presented.

2. Experimental

To observe the Mössbauer effect by detecting conversion electrons were used different devices [2]. The proportional counter is the most used and it represents a cheap solution.

In our institute have been developed some proportional counters for conversion Mössbauer spectroscopy: detectors for conversion electron and transmission Mössbauer spectroscopy [4-5], detector for conversion X-ray and transmission Mössbauer spectroscopy (CXMS) [6], detector assembly for simultaneous

conversion electron, conversion X-ray and transmission Mössbauer spectroscopy [5], versatile flow-gas proportional counter for surface Mössbauer spectroscopy [7]. All detectors are flow-gas type and operating at room temperature. Their construction permits for all detectors to realize simultaneous transmission and conversion measurements. The background due to photoelectrons is minimised by using low- Z materials as much as possible. The sample holder allows an easy manipulation of a sample, outside the detector and sample can always be repositioned in a reproducible manner with respect to the detector body. We have used for detectors an economical shielding which consists of a combination of lead, copper and steel disks. In order to absorb unfavourable KX-rays from the source, a plexiglas filter is placed in front of the shielding.

The versatile flow-gas proportional counter for surface Mössbauer spectroscopy [7] represent a synthesis of our experience in the development of flow-gas proportional detectors for surface studies. The main improvements obtained by new design are: the height of the detection volume can be changed in large limits from 1 to 38 mm, the detection volume can be choose symmetrical or not in respect with anode plan, the anode changing is easily and different anode configuration can be used. By changing the volume detection and flow gas it is possible to make measurements by electron, X-ray detection or gamma-ray detection. The diagram of this detector is present in figure 1. After our knowledge, for the first time, was realized the detection of low energy X-ray for ^{119}Sn and obtained a Mössbauer spectrum. The detectors were inserted into a Mössbauer spectrometer. For conversion electron detection a 94% He + 6% CH₄ or 99% He + 1% C₄H₁₀ mixtures was used and for X-ray a 90% Ar + 10% CH₄ mixture. The gas flow rate can be set in the range of 50 – 1000 cm³/hour by a flowmeter working at a pressure of about 0.1 MPa.

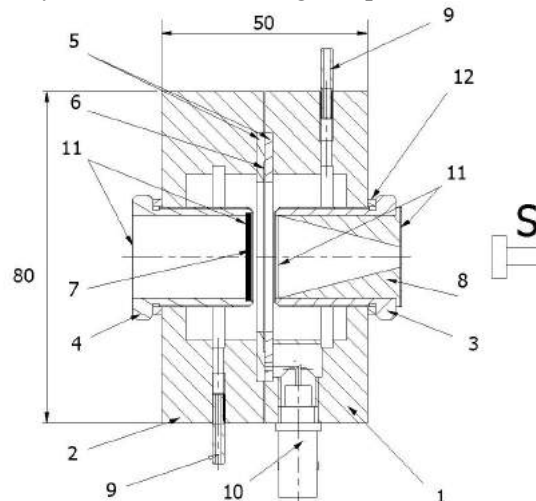


Fig. 1. The cross section of the versatile flow-gas proportional counter, 1 and 2 main parts of the counter, 3 input piece, 4 sample holder, 5 teflon insulator, 6 anodic ring, 7 sample, 8 collimator, 9 gas connection, 10 high voltage connector, 11 mylar windows, 12 tightness piece, S Mössbauer source.

The spectrometric chain has been supplemented with additional modules such as to allow simultaneous recording of spectra. To test the performance of the counters, Mössbauer measurements were carried on reference samples as: a 25 μm thick stainless steel sample (type 310), a rhodium foil 30% enriched in ^{57}Fe , β -tin foil, Eu_2O_3 powder deposited on substratum. The parameters of Mössbauer spectra have been calculated using a specialized, computer-fitting program, which assumes Lorentzian line resonances.

3. Results

Were carried many studies by conversion electron Mössbauer spectroscopy (CEMS) for different materials in the nano range dimension scale. So were investigated, for example: ^{57}Fe doped anatase nanoparticles [8], [9], Eu doped yttrium vanadate nanoparticles [10], the structural and magnetic properties of different films: $\text{Fe}_{81}\text{B}_{13.5}\text{Si}_{3.5}\text{C}_2$ films [11], Fe-ion-implanted Cu and Ag films [12], MnZnTi and NiZn ferrite films [13], the effects induced, mainly in surface, by pulsed radio frequency annealing of $\text{Fe}_{81}\text{B}_{13.5}\text{Si}_{3.5}\text{C}_2$ (Metglass 2605 SC) glass [14-17], nanocrystallization of the $\text{Fe}_{87}\text{Zr}_6\text{B}_6\text{Cu}_1$ [18], corrosion processes [19-25], superficial characterization of α -iron oxides obtained by hydrothermal synthesis [26], the surface phase composition of bulk and thin films samples of SnSe_2 [27], characterization of Fe-C steel under electrolytic galvanisation [28] etc. Some of them are shortly described below.

Low carbon Fe-C steel surface has been studied before and after electrolytic galvanization. The corrosion products formed under atmospheric conditions on the Fe-C steel were identified and characterised by, mainly, Mössbauer spectroscopy [28]. Figure 2 show the Mössbauer spectra of the initial sample, figure 3 show the sample ready for deposition, together with the computer fit (continuous lines).

The surface measurements on initial sample prove a marked corrosion: a coating with a considerable thickness and a complex composition. Hematite is the main compound of the outermost layer (Fig. 2e). Its Mössbauer parameters are practically the same with those given in literature. The second compound in the outermost layer is magnetite with a normal stoichiometry as in different references. In the outermost layer there is also goethite. The Mössbauer parameters for goethite have a great dispersion. The reduced hyperfine magnetic field of goethite compared with well-crystallized goethite (around 380 kOe), can be generally assigned to varying crystallinity of goethite and/or small particles. Poor crystallinity and substitution may modify the spectrum of goethite to such an extent that characterization must be carried out at low temperatures. According to the level diagram of Gibbs free energies of formation for some corrosion products of iron, α - FeOOH is a level in the transition to α - Fe_2O_3 . Also a corrosion product can exist in the outermost layer at sensibility limit of the method. Its presence is suggested by smoothing the spectrum.

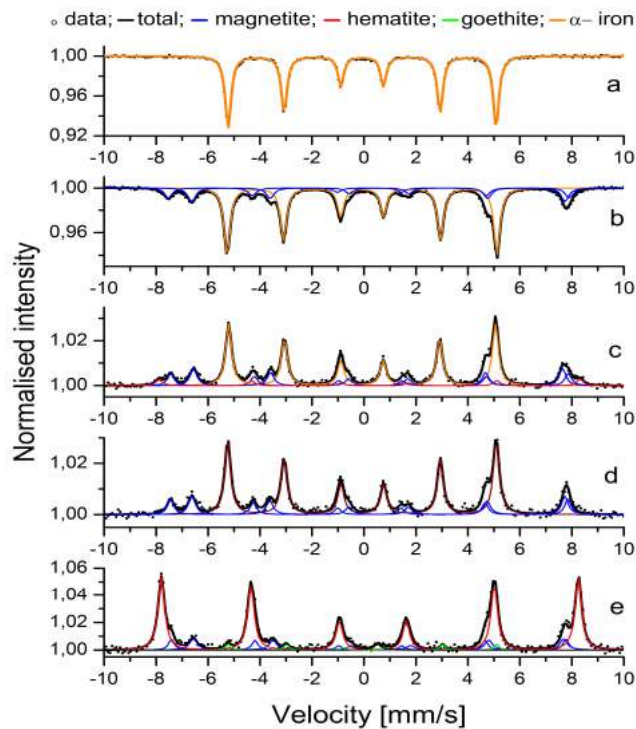


Fig. 2. Mössbauer spectra of the initial sample
 (a) from bulk; (b) of surface scrapped layer; (c) by CXMS without filter; (d) by CXMS with filter;
 (e) by CEMS.

CEMS spectra indicate a corrosion layer thickness greater than 250 nm. The spectrum of steel substrate was not evidenced. The surface spectra obtained by CXMS without electron filter (Fig. 2c) give the integral information about superficial corrosion layer. The magnetite and hematite are the compounds of the layer. Magnetite is now the main compound of the corrosion layer. The using of the electron filter hides the hematite presence (Fig. 2d). Also the hematite is not present in the surface sample collected by scape method (Fig. 2b). The data obtained for sample collected by scape method are very closely to those obtained by CXMS with electron filter. All CXMS spectra evidenced the steel substrate. The spectra of the samples ready for electro deposition (Fig. 3) show the moving off the corrosion layer and the single presence of α -Fe. The Fe sextet has hyperfine parameters, practically the same as for the initial sample. The intensities of the second and fifth peaks of these sextets with respect to the third and fourth peaks, in CEMS spectra (Fig. 3a), showed that the directions of the γ -ray and magnetic moments were nearly perpendicular and thus indicate a magnetic anisotropy at surface samples. The magnetic moments of iron tend to be orientated in surface plane. By contrast, the TMS and CXMS spectra showed that the magnetic moments

inside the sample were in a random arrangement. The anisotropy found in superficial layer of around 250 nm thickness, by CEMS spectra, is obtained, mainly, due to the preparation process of steel sheets for galvanization.

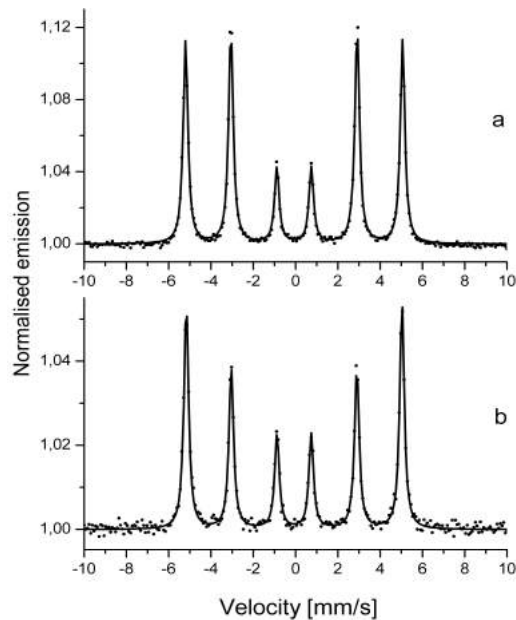


Fig. 3. Mössbauer spectra of the sample ready for electro deposition: (a) by CEMS; (b) by CXMS without filter.

Fe based nanocrystalline alloys have been exhaustively studied in the last years due to their excellent soft magnetic properties. The crystallisation process of the $\text{Fe}_{87}\text{Zr}_6\text{B}_6\text{Cu}_1$ sample has been studied by means of, transmission Mössbauer spectrometry, CEMS and x-ray diffraction [18]. $\text{Fe}_{87}\text{Zr}_6\text{B}_6\text{Cu}_1$ amorphous ribbon were obtained by the melt spinning technique. The surface of the as-quenched ribbon was subsequently polished to remove any possible residual surface crystal. One-hour isothermal treatments at 350, 475 and 575 °C were performed in a differential thermal analyser apparatus in an Ar atmosphere. In figure 4 are presented the transmission Mössbauer spectra and the obtained ones by CEMS technique for the as-quenched sample and samples annealed at 350°C and 575°C. As it can observe, there are no great differences between the spectra corresponding to the as-quenched sample. The directions of the γ -ray and the magnetic moments are nearly perpendicular in the annealed samples, so there is a magnetic anisotropy on the surface of the samples, revealed by CEMS spectra. The experimental results show different grades of crystallisation depending on the depth of the layer studied. The crystallisation process begins on the surface of the sample and extent with annealing temperature to the interior the sample.

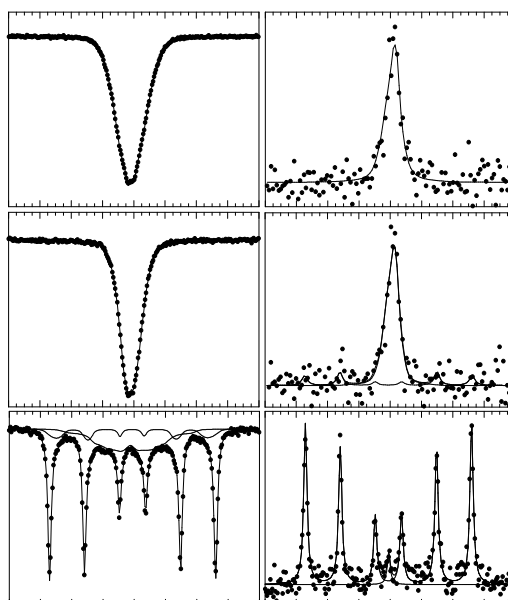


Fig. 4. Mössbauer spectra and fittings for the as-quenched sample and samples annealed at 350 and 575°C.

Nanomaterials based on various chalcogenides have strong implications in many applications including biology and medicine for cancer treatment, typhoid fever and plant growth promotion. Tin chalcogenides SnX_2 and SnX , where $\text{X}=\text{S}$, Se or Te , present a particular interest for their electronic properties and applications in gas sensors. They belong to amorphous and glassy chalcogenides, materials which are sensitive to light and other radiations. Structure and Mössbauer measurements on SnSe_2 bulk and thin films were performed [27]. SnSe_2 , bulk samples, was prepared by mixing corresponding amounts of Sn and Se powder (high purity grade) in sealed quartz ampoule. The thin films were deposited by pulsed laser deposition (PLD) and pulsed electron deposition (PED). In Fig. 5 are presented the CEMS spectra obtained on SnSe_2 films deposited by two methods: PLD and PED deposition methods. The main component of the film spectra can be assigned to SnSe_4 species by its isomer shift values: 1.69 and 1.66 s. These species are known as tetrahedral Zintl anions $[\text{SnSe}_4]$. It is possible that studied films to be built from isolate SnSe_4 tetrahedra stabilized by atoms occupying intermediated positions. A similar process met in mesostructured chalcogenide-based materials with long-range order and semiconducting properties using molecular building blocks, linked by metal ions and surfactant molecules. The higher line width of the main component can be explained by the fact that SnSe_4 have tin environments slightly distorted from the basic tetrahedral symmetry. The compound SnSe there is present

in the both films in a small amount. The increased line width of the SnSe is explained by its quadrupole splitting with a value around 0.65 mm/s.

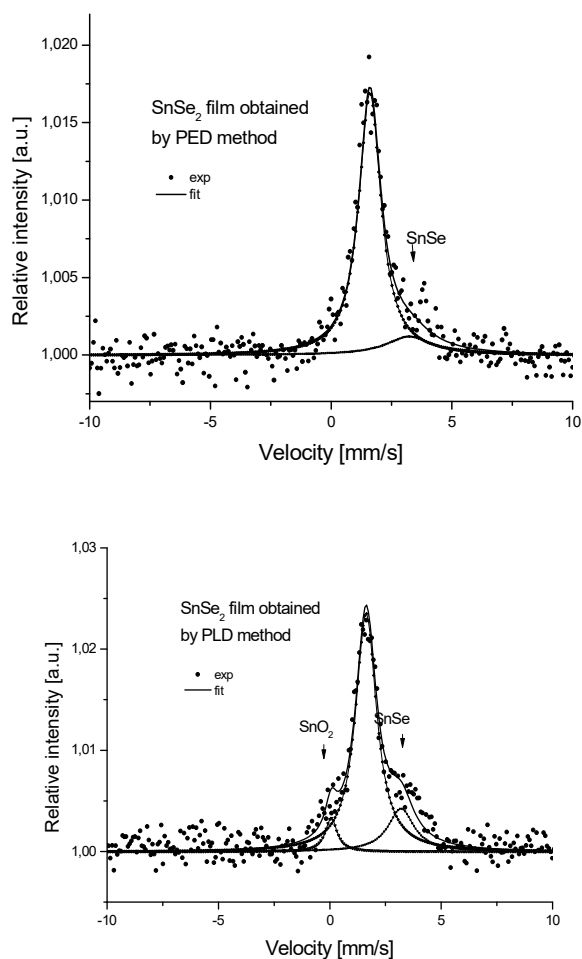


Fig. 5. Conversion electron Mössbauer spectroscopy spectra of SnSe₂ films obtained by PLD and PED deposition.

The higher line width of the SnSe in the PLD film suggest a light structure distortion of the SnSe compound with orthorhombic structure. The SnSe presence can be explained by the occurrence of the reaction: $\text{SnSe}_2 \rightarrow \text{SnSe} + \text{Se}$ in the deposition process. In the film spectrum obtained by PLD deposition we identify a third component, assigned to SnO₂ oxide. The oxide is localized at the film surface, the most probably, showing an oxidation in air atmosphere of the film. We believe, according to our results, that by PED deposition method a better film is obtained. The arguments for the affirmation are: a higher proportion of the main component,

a lower line width of the main component, a lower line width of the SnSe component, the absence of the SnO₂ oxide.

YVO₄:Eu³⁺ is a strong luminescent material, largely used as red phosphor in high pressure mercury lamps. The recent studies show that nanosized YVO₄:Eu³⁺ is a significant promise for plasma display panels (PDP). Eu³⁺ ion substitutes the Y³⁺-site. Using Eu as sensitive probe for Mössbauer spectroscopy, the local changes induced by the thermal treatments of YVO₄ nanocrystals are evidenced [10]. YVO₄:Eu³⁺-nanocrystals (with nominal 5 at.% Eu) have been obtained by the precipitation procedure. Mössbauer measurements were performed at room temperature by standard transmission and electron backscattering (CEMS) techniques. A background correction and a smoothing procedure of the spectra were performed before the fitting runs. The Mössbauer experimental spectra of YVO₄ nanopowders annealed in air at different temperatures and fitting patterns are plotted in figure 6 (backscattering spectra).

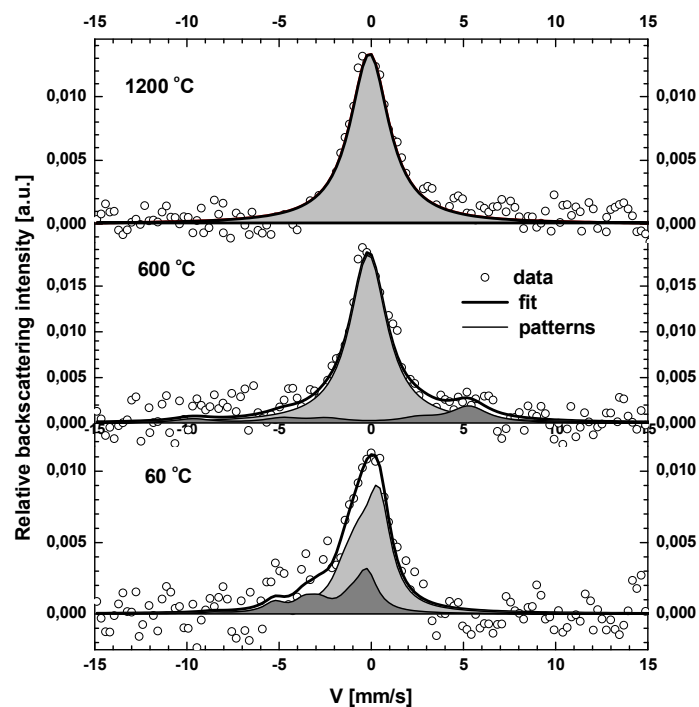


Fig. 6. The experimental backscattering spectra of the YVO₄:Eu powders annealed at various temperatures and fitting patterns

Up to 700 °C, the Mössbauer spectra consist in two main contributions: a central broad ($\sim 8 \text{ mm/s} \div 9 \text{ mm/s}$) as preponderant ($\sim 65\%$) line-resonance (A) and a less large ($\sim 4 \text{ mm/s} \div 5 \text{ mm/s}$) and less intense ($\sim 35\%$), resonance (B), at around $v \in [5 \text{ mm/s} \div 7 \text{ mm/s}]$. This behaviour can be ascribed to the presence of Eu ions in

different possible micro-environments in $\text{YVO}_4\text{:Eu}$ structure. The two different micro-environments of ^{151}Eu , correspond to different distorted oxygen polyhedrons ($|eQ_{7/2}V_{zzA}| < |eQ_{7/2}V_{zzB}|$) of trivalent Eu-ions. As the annealing temperature increases, the feature of the spectra changes too. The intensity of the B doublet decreases up to its disappearance and A doublet becomes more symmetric at $T_0 \sim 700^\circ\text{C}$. The backscattering spectra suggest a higher distortion of the Eu neighborhood at surface. The best fit of transmission spectra for the sample annealed at $T > 700^\circ\text{C}$ was obtained considering only one pattern with hyperfine parameters values much closed to the doublet A parameters. The increase of the particle size diminishes the surface contribution to the Mössbauer spectrum, consequently the volume contribution becomes dominant at the annealing temperature of $T > 700^\circ\text{C}$. The fit results for the annealed samples revealed a critical temperature $T_0 \approx 700^\circ\text{C}$, suggesting a transition state in the growth process of $\text{YVO}_4\text{:Eu}$ crystallite.

3. Conclusions

The possibility to make measurements in the nano or micro range by Mössbauer spectroscopy using ^{57}Fe , ^{119}Sn and ^{151}Eu Mössbauer isotopes was proved. Measurements were made with different flow gas detectors in a backscattering geometry by detection of electron or X rays.

Nanocharacterization measurements were realized on the following samples: ^{57}Fe doped anatase nanoparticles, $\text{Fe}_{81}\text{B}_{13.5}\text{Si}_{3.5}\text{C}_2$ (Metglass 2605 SC) glass, $\text{Fe}_{81}\text{B}_{13.5}\text{Si}_{3.5}\text{C}_2$ films, Fe-ion-implanted Cu and Ag films, MnZnTi and NiZn ferrite films, α -iron oxides obtained by hydrothermal synthesis, $\text{Fe}_{87}\text{Zr}_6\text{B}_6\text{Cu}_1$, carbon steel corroded in diluted ammoniacal media or HCl solutions in presence or absence of organic corrosion inhibitors, carbon steel used in electrolytic galvanisation, ^{151}Eu yttrium vanadate nanoparticles, thin films samples of SnSe₂, etc.

References

- [1] Mössbauer R.L., *Nuclear Resonance Fluorescence of gamma Radiation in ^{191}Ir* , Z. Physik., **151**, 1958, p. 124-143.
- [2] Belozerskii G.N., *Moessbauer Studies of Surface Layers*, (Studies in Physical and Theoretical Chemistry Series; 81), Elsevier Science, Amsterdam, Hetherlands, 1993.
- [3] Long G.J., Grandjean F., eds., *Moessbauer Spectroscopy Applied to magnetism and Materials Science*, vol. 2, PlenumPress, New York, USA, 1996.
- [4] Bibicu I., Rogalski M.S., Voiculescu Gh., Nicolescu G., Barb D., *Proportional counter for conversion and transmission Mössbauer spectroscopy*, Rev. Roum. Phys., **37**, 1992, p. 315-317.
- [5] Bibicu I., Rogalski M.S. and Nicolescu G., *A detector assembly for simultaneous conversion electron, conversion X-ray and transmission Mössbauer spectroscopy*, Meas. Sci. Technol., **7**, 1996, p. 113-115.
- [6] Bibicu I., Rogalski M.S., Nicolescu G., *Toroidal proportional detector for conversion X-ray and transmission Mössbauer spectroscopy*, Nuclear Instruments and Methods in Physics, Research B, **94**, 1994, p. 330-332.

- [7] Bibicu I., Nicolescu G., Cretu C., *A versatile gas-flow proportional counter for Mössbauer spectroscopy*, *Hyperfine Interactions*, **192**, 1, 2009, p. 85-91.
- [8] Grecu M.N., Constantinescu S., Tarabasanu- Mihaila D., Ghica D., Bibicu I., *Spin dynamics in ^{57}Fe -doped TiO_2 anatase nanoparticles*, *Phys. Status Solidi B* **248**, 12, 2011, p. 2927-293, DOI 10.1002/pssb.201147124.
- [9] Bibicu I., Constantinescu S., Tarabasanu-Mihaila D., Grecu M.N., *CEMS measurements on low ^{57}Fe doped anatase nanoparticles*, *Romanian Reports in Physics*, **68**, 4, 2016, p. 1506-1512.
- [10] Bibicu I., Constantinescu S., Diamandescu L., Voiculescu A.M., Cotoi E., *Mössbauer spectroscopy study on $\text{YVO}_4:\text{Eu}$ luminescent material*, *Rom. Rep. in Phys.* **66**, 4, 2014, p. 1012-1017.
- [11] Rogalski M.S., Jackson T.J., Bibicu I., Palmer S.B., *Deposition of $\text{Fe}_{81}\text{B}_{13.5}\text{Si}_{3.5}\text{C}_2$ films by excimer laser ablation and their structural investigation*, *Journal of Physics D*, **27**, 1994, p. 2167-2170.
- [12] Pereira de Azevedo M.M., Sousa J.B., Mendes J.A., Almeida B.G., Rogalski M.S., Pogorelov Yu.G., Bibicu I., Redondo L.M., da Silva M.F., Jesus C.M., Marques J.G., Soares J.C., *Magnetization and magnetoresistance in Fe-ion-implanted Cu and Ag thin films*, *Journal of Magnetism and Magnetic Materials*, **173**, 1997, p. 230-240.
- [13] Amado M.M., Rogalski M.S., Guimaraes L., Sousa J.B., Bibicu I., Welch R.G., Palmer S.B., *Magnetic properties of NiZn and MnZn ferrite films deposited by laser ablation*, *J. Appl. Phys.*, **83**, 11, 1998, p. 6852 – 6854.
- [14] Rogalski M., Bibicu I., *Surface short range order induced by RF annealing $\text{Fe}_{81}\text{B}_{13.5}\text{Si}_{3.5}\text{C}_2$ glass*, *Materials Letters*, **13**, 1992, p. 32-34.
- [15] Bibicu I., Rogalski M.S., Nicolescu G., *Transmission and conversion electron Mössbauer investigation of $\text{Fe}_{81}\text{B}_{13.5}\text{Si}_{3.5}\text{C}_2$ glass under RF thermal treatment*, *Phys. Stat. Sol. (b)*, **178**, 1993, p. 459-464.
- [16] Rogalski M.S., Bibicu I., Sorescu M., *CEMS investigations of surface hyperfine interactions in $\text{Fe}_{81}\text{B}_{13.5}\text{Si}_{3.5}\text{C}_2$ glass*, *Hyperfine Interactions*, **92**, 1994, p. 1317-1321.
- [17] Rogalski M.S., Bibicu I., *CEMS, CXMS and transmission Mössbauer investigation of the RF isochronal annealing of $\text{Fe}_{81}\text{B}_{13.5}\text{Si}_{3.5}\text{C}_2$ glass*, *Phys. Stat. Sol (b)*, **195**, 1996, p. 531-536.
- [18] Bibicu I., Garitaonandia S., Plazaola F., Apinanz E., *X-ray diffraction, transmission Mössbauer spectrometry and conversion electron Mössbauer spectroscopy studies of the $\text{Fe}_{87}\text{Zr}_6\text{B}_6\text{Cu}_1$ nanocrystallization process*, *Journal of Non-Crystalline Solids*, **287**, 2001, p. 277-281.
- [19] Bibicu I., Samide A., Preda M., *Steel corrosion in diluted ammonia solutions studied by Mössbauer spectrometry*, *Materials Letters*, **58**, 21, 2004, p. 2650-2653.
- [20] Samide A., Bibicu I., Rogalski M., Preda M., *Surface study of the corrosion of carbon steel in solutions of ammonium salts using Mössbauer spectrometry*, *J. Radioanal. Nucl. Chem.*, **261**, 3, 2004, p. 593-596.
- [21] Samide A., Bibicu I., Rogalski M., Preda M., *A study of the corrosion inhibition of carbon-steel in diluted ammonia media using 2-mercapto-benzothiazol (MBT) by Mössbauer*, p. 127-136.
- [22] Samide A., Bibicu I., Rogalski M.S., Preda M., *Surface study of the corrosion inhibition of carbon steel in diluted ammonia media using N-ciclohexil-benzothiazole-sulphenamida*, *Corrosion Science*, **47**, 5, 2005, p. 1119-1127.
- [23] A. Patru, I. Bibicu, M. Agiu, M. Preda, B. Tutunaru, *Surface study of the corrosion inhibition of carbon steel in diluted ammonia media using N-ciclohexil-benzothiazole-sulphenamida*, *Materials Letters*, **62**, 2008, 320- 322.
- [24] Samide A., Bibicu I., Turcanu E., *Surface analysis of inhibitor films formed by N-(2hydroxybenzilidene) thiosemicarbazide on carbon steel in acidic media*, *Chemical Engineering Communications*, **196**, 2009, p. 1008-1017.
- [25] Samide A., Bibicu I., *Kinetics corrosion process of carbon steel in hydrochloric acid in absence and presence of 2-(cyclohexylaminomercapto) benzothiazole*, *Surface and Interface Analysis*, **40**, 2008, p. 944-952.
- [26] Diamandescu L., Mihaila-Tarabasanu D., Popescu-Pogrion N., Totovana A., Bibicu I., *Hydrothermal synthesis and characterization of some polycrystalline α – iron oxides*, *Ceramics International*, **25**, 1999, p. 689 – 692.

[27] Bibicu I., Lőrinczi A., Velea A., Sava F., Popescu M., *Structure and Mössbauer measurements on SnSe₂ bulk and thin films*, Optoelectronics and Advanced Materials-Rapid Communications, **4**, 10, 2010, p. 1568-1571.

[28] Bibicu Ion, Bulea Caius, Diamandescu Lucian, Rus Vasile, Popescu Traian, Mercioniu Ionel, *Characterization of surface and interface of Fe-C steel under electrolytic galvanisation*, Proceedings of the Romanian Academy – series A; **19**, 3, 2018, p. 423-430.